Computer Networks 101 (2016) 19–28

Contents lists available at ScienceDirect

Computer Networks

journal homepage: www.elsevier.com/locate/comnet

A grid-based joint routing and charging algorithm for industrial wireless rechargeable sensor networks

Guangjie Han[a,b,*], Aihua Qian[a], Jinfang Jiang[a], Ning Sun[a], Li Liu[a]

[a] Department of Information & Communication Engineering, Hohai University, Changzhou 213022, China
[b] Changzhou Key Laboratory of Sensor Networks and Environmental Sensing, Changzhou 213022, China

ARTICLE INFO

Article history:
Received 31 July 2015
Revised 30 October 2015
Accepted 9 December 2015
Available online 6 January 2016

Keywords:
IWRSNs
grid-based
joint routing and charging
proactively charging

ABSTRACT

Wireless charging techniques provide a more flexible and promising way to solve the energy constraint problem in industrial wireless rechargeable sensor networks (IWRSNs). Although considerable research has been done on wireless charging algorithms, most of it only focuses on passively replenishing nodes having insufficient energy. In this paper, we propose a grid-based joint routing and charging algorithm for IWRSNs to solve the charging problem in a proactive way. On the one hand, a new routing protocol is designed according to charging characteristics of the charger to achieve local energy balance. On the other hand, different charging times are allocated at different charging points on the basis of energy consumption caused by the routing process to achieve global energy balance. Simulation results verify superiority of our proposed algorithm in solving the balancing energy problem and improving survival rates of nodes.

1. Introduction

Recently, industrial wireless sensor networks (IWSNs) have become widely applied to many industrial fields, such as the production automation, real time telemetry, smart homes, large-scaled structures etc. [1–5]. IWSNs are composed of energy limited sensor nodes, which are usually powered by a battery. It is quite expensive to replace all nodes having used all their power with new ones, especially in large-scale sensing areas. Accordingly, some studies, such as, for examples, [6–8], attempt to solve the energy constraint problem by designing energy-saving routing protocols. The protocols can prolong the network lifetime to a certain extent, but cannot fundamentally resolve the energy constraint problem. Recent technological advances in wireless charging technologies inspire researchers to apply them to IWSNs, which can be used to supply sensor nodes with electricity. In IWRSNs, a mobile charger is equipped with a wireless energy transmitting module, and sensor nodes are equipped with wireless energy receiving modules. Thus, the mobile charger can replenish energy of sensor nodes wirelessly.

A key issue related to IWRSNs is how to design a charging strategy to prolong the lifetime of nodes as much as possible. So far, there have been a certain amount of studies on wireless charging related to wireless rechargeable sensor networks (WRSNs) [9–13], which are also suitable for IWRSNs. The main idea of existing charging algorithms is to replenish energy in nodes that are short of energy. In other words, these algorithms adopt a passive charging method: energy is only passed to sensor nodes having little energy left. In this paper, we propose a grid-based joint routing and charging algorithm for IWRSNs to solve the energy constraint problem in a proactive way. First, instead of passively replenishing energy for nodes, we design a new routing protocol to avoid energy unbalance as much as possible. Further, we divide the network

* Corresponding author. Tel.: +8651985191841; fax: +8651985191833.
E-mail addresses: hanguangjie@gmail.com, hanguangjie@hhu.edu.cn (G. Han), bettyhhuc@gmail.com (A. Qian), jiangjinfang1989@gmail.com (J. Jiang), sunn2001@hotmail.com (N. Sun), liulihhuc@gmail.com (L. Liu).

http://dx.doi.org/10.1016/j.comnet.2015.12.014
1389-1286/

into many small grids, the vertices of which are charging points for a mobile charger to sojourn and deliver energy to nodes. Moreover, the charging time at each point is determined by the energy consumption rate of nodes around it to achieve more balanced energy distribution.

The main contribution of this paper is that we propose a grid-based joint routing and charging algorithm, and verify its effectiveness by comparing its charging performance to the S-CURVES(ad) proposed in [14]. Since the goal of charging is to replenish energy and improve survival rate of nodes, the average residual energy, standard deviation of residual energy, and survival rate are chosen as evaluation parameters in this paper.

The remainder of the paper is organized as follows. Section 2 summarizes current developments in the field of charging algorithms for WRSNs. Section 3 describes our grid-based joint charging and routing algorithm in detail. Section 4 presents simulation results followed by particular analysis. Section 5 concludes and suggests future work.

2. Related work

Recent developments in wireless charging technologies have greatly contributed to the emergence of IWRSNs. In this paper, we propose a charging algorithm on the basis of the wireless charging model presented in [15]. We assume the IWRSN is built from the industrial wireless identification sensing platform (WISP) and commercial RFID readers. In what follows, we refer to the RFID reader as a charger, for simplicity. According to this charging model, the relationship between the transmission power of transmitter P_t and received power of receiver P_r can be formalized as follows:

$$P_r = \frac{G_s G_r \eta P_t}{L_p} \left(\frac{\lambda}{4\pi (d_0 + \beta)} \right)^2 \quad (1)$$

where G_s and G_r are antenna gains of the transmitter and receiver, respectively. η is the rectifier efficiency, L_p is the polarization loss, λ is the wavelength of the signal, β is a parameter used to adjust the Friis' free space equation for short distance transmissions, and d_0 is the distance between the transmitter and receiver. In our case, the transmitter is a charger, and the receiver is a sensor node. To ease the description of the equation, we reformulate (1) as $P_r = \frac{\alpha}{(d+\beta)^2}$ where $\alpha = \frac{G_s G_r \eta P_t}{L_p} (\frac{\lambda}{4\pi})^2$. Experiments conducted in [15] show $\alpha = 4.32 \times 10^{-4}$, $\beta = 0.2316$. We can see from this formula that the received power of nodes decreases rapidly with the increase in distance between the transmitter and receiver. That is, if the charger is too far away from the sensor node, the wireless charging power is too low to be harvested. Therefore, we assume that there exists a distance threshold, denoted by the charging range R, beyond which nodes cannot be charged. We set R to be $5m$ in this paper.

So far, there have been a certain number of studies on charging strategies in WRSNs [11–16]. However, the existing charging algorithms have not been classified. In this paper we classify the existing charging algorithms into two groups based on the mobility state of chargers: (1) static chargers, such as algorithms proposed in [16], (2) mobile chargers such as algorithms proposed in [17–21]. We then provide a brief introduction for some of them.

In [15], Shibo He et al. study the energy provisioning problem in WRSNs, with the focus on designing a strategy to deploy as less RFID readers as possible. First, by conducting experiments, the authors obtain a wireless recharging model. Then, two forms of solutions, namely, point provisioning and path provisioning, are proposed. In both solutions, the authors estimate a lower bound of the optimal solution, and provide an approximation ratio of the proposed solution to this lower bound presenting a detailed mathematical derivation. Simulation results show that the mobility of WISP tags can be further exploited to solve the energy provisioning problem. In addition, the deployed methods proposed in [15] can reduce the number of readers effectively.

Richard Beigel et al. [17] propose a scheme for optimal scheduling of multiple mobile chargers. The authors study the mobile charger coverage problem of sensor nodes distributed on a 1-dimensional line and ring. They provide an optimal solution with linear complexity to address two pivotal problems: the minimum number of mobile chargers needed, and the best schedule for multiple chargers in terms of trajectory planning. Unfortunately, the charging strategy proposed in this paper is aimed for 1-D lines and rings, being not scalable in common WSNs.

Guangjie Han et al. [14] propose four traveling paths for mobile chargers, and compare charging performance. The paths are the SCAN, HILBERT, S-CURVES(ad) and Z-curve, which are all space-filling curves and static traveling paths. In [14], the charging times at charging points are equal. Comprehensive comparison is made to measure the charging performance of different traveling paths in terms of the traveling length, number of alive nodes over time, traveling efficiency, and charging latency. Simulation results show that the S-CURVES(ad) outperforms the Z-curve in charging latency and traveling efficiency. In addition, its performance in improving the lifetime of nodes and traveling efficiency is better than that of the SCAN and HILBERT. It benefits from the fact that the S-CURVES(ad) has the largest number of stop locations, and the shortest traveling length.

In [20], Lingkun Fu et al. propose a charging scheme for WRSNs to minimize charging delays. The main contribution of this paper is that the authors plan an optimal movement strategy of the RFID reader to guarantee that the time to charge all nodes in the network is minimized. An optimal solution using linear programming is proposed, but the computational complexity of the method is relatively high. To further optimize this solution, the authors introduce a heuristic solution using an approximation ratio by discretizing charging power into a 2-D space. Simulation results verify the effectiveness of the heuristic solution in terms of charging delays.

In view of the fact that the charging range of the charger is very limited, one needs many chargers to meet the energy demand of nodes, especially when the network is large-scale. Accordingly, in this paper, we only consider the case with one mobile charger. The majority of pioneering works on the mobile charging problem focused on replenishing energy in nodes having lower energy, which

leads us to design a joint routing and charging algorithm. Inspired by the path planning algorithms proposed in [22–24], we design a new path planning method for a mobile charger, which aims to achieve better charging performance. The main characteristics of our proposed algorithm include two aspects: designing routing protocol according to the amount of energy the nodes can obtain, and deciding charging time at each charging point according to energy consumption caused by the routing protocol.

3. Grid-based joint routing and charging algorithm

Before we introduce the grid-based joint routing and charging algorithm in detail, we provide a brief introduction of the network model. In industrial scenarios, numerous sensor nodes are deployed in the network, which take responsibility to sense data from environments, and cooperate to transmit data to the Base Station. As shown in Fig. 1, the sensor nodes are densely and uniformly deployed in the monitored square area with side length L. We assume that all sensor nodes are aware of their locations. Every T seconds, nodes transmit data packets they sensed as well as information about their energy level to the Base Station. The energy consumption model of nodes proposed in [25] is adopted in this paper. Transmission of n_b bits at a distance d_0 consumes $n_b(E_{elec} + E_{amp} \times d_0^n)J$. Reception of n_b bits consumes $n_b \times E_{elec}J$. $n = 2$, E_{elec} and E_{amp} are constants. There is a mobile charger, which first charges itself at the service station, and then traverses the whole network to provide energy to sensor nodes. Its moving speed is v (m/s). It can directly communicate with the Base Station at anytime and anywhere.

The whole network is divided into many grids of the same size. The grids are defined as charging grids, and the vertices of the grids are defined as charging points where the mobile charger stops to replenish energy. The size of each charging grid is d. For simplicity, d is divisible by L. Fig. 2(a) shows the corner case. A, B, C and D represent charging points, and the green circle represents the charging range. Clearly we obtain: $\sqrt{2}d \le 2R$ (i.e., $d \le \sqrt{2}R$). The time that the mobile charger spends at different charging points may be different according to the charging strategy. After traversing the whole network once, the charger comes back to the service station to recharge its battery and get ready for the next tour.

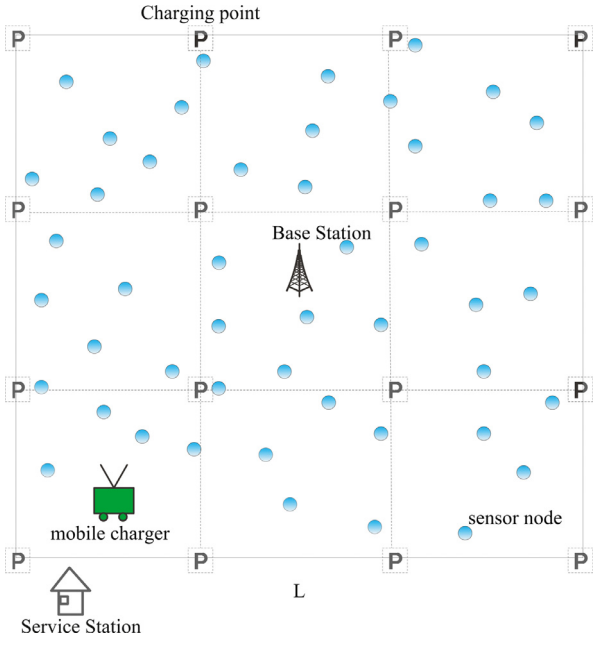

Fig. 1. Network model.

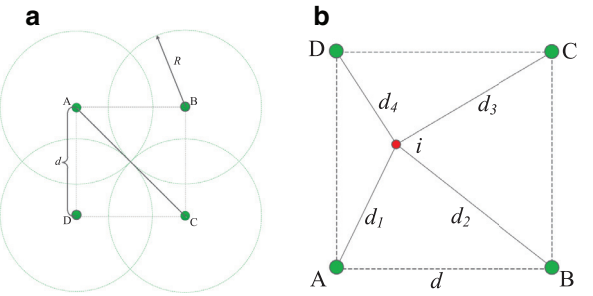

Fig. 2. Charging grid and power calculation.

Generally, our grid-based joint routing and charging algorithm contains two phases. In the first phase, a new routing protocol is proposed according to the charging characteristics of the charger to balance energy consumption of sensor nodes locally (within the charging grid). In the second phase, the charging strategy of the mobile charger is designed. Specifically, the strategy includes the path of travel and charging times at charging points. The goal of designing the charging strategy is to solve the energy unbalance problem caused by the proposed routing protocol. In the second phase, energy balance over the whole network can be achieved globally. In the next subsections, we discuss the two phases in detail.

3.1. Routing protocol

Being aware of the side length of each charging grid d, each node in the network can determine which charging grid it belongs to. As shown in Fig. 2(b), there is a node i with coordinates (x_i, y_i), and the vertices of its charging grid are A, B, C and D. Their coordinates can be calculated as follows:

$$\left(\lfloor\frac{x_i}{d}\rfloor d, \lfloor\frac{y_i}{d}\rfloor d\right), \left(\lceil\frac{x_i}{d}\rceil d, \lfloor\frac{y_i}{d}\rfloor d\right), \left(\lfloor\frac{x_i}{d}\rfloor d, \lceil\frac{y_i}{d}\rceil d\right), \left(\lceil\frac{x_i}{d}\rceil d, \lceil\frac{y_i}{d}\rceil d\right) \quad (2)$$

Each node can calculate the distances to the charging points A, B, C and D. They are d_1, d_2, d_3, and d_4, respectively. Furthermore, the power that the node i can obtain P_{r_i} is the sum of energy it obtains from the four charging points A, B, C and D. Thus, P_{r_i} can be calculated as follows according to the formulation introduced in Section 2:

$$P_{r_i} = \alpha\left(\frac{1}{(d_1+\beta)^2} + \frac{1}{(d_2+\beta)^2} + \frac{1}{(d_3+\beta)^2} + \frac{1}{(d_4+\beta)^2}\right) \quad (3)$$

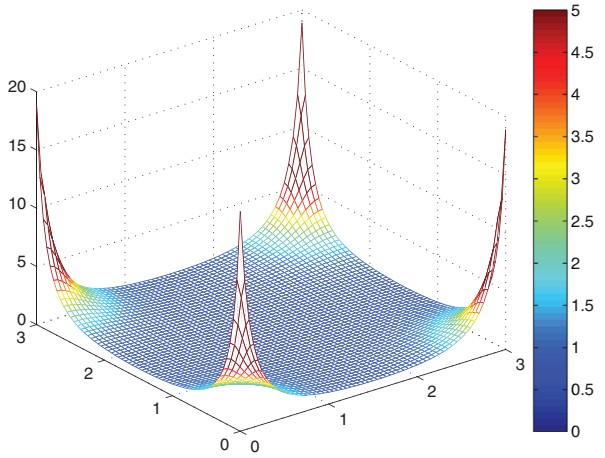

Fig. 3. Energy distribution when d=3m.

We conducted experiments using MATLAB to see the provisioning energy distribution in the grid area. Here we simulate the case $d = 3m$. As we can see in Fig. 3, the provisioning energy distribution is far from being balanced: the nodes near charging points can obtain much more energy than the nodes close to the center region of the grid. We note that as d decreases, such unbalance is alleviated to some extent. Unfortunately, it results in another problem: the mobile charger has to stop at more charging points, and the traveling length becomes longer. When energy unbalance in the charging grid cannot be avoided, we design a new routing protocol aimed at balancing energy in the grid area. The main idea is to preferentially choose sensor nodes which can get more energy to be relay nodes, since the relay nodes undertake more communication tasks and consume more energy. Some definitions of the protocol are given as follows.

Preferred circle: Preferred circles are the circles whose centers are charging points, with radius r_1. A preferred circle is denoted by $C_p(V)$, where V represents the center of the preferred circle as well as a charging point. The nodes in preferred circles are the preferred choices to be relay nodes, because they have closer distance to the charging points, and can obtain more energy. As shown in Fig. 4, a sensor node i in the preferred circle V_1 is denoted by $i \in C_p(V_1)$.

Extended circle: Extended circles are the circles whose centers are charging points, with radius r_2 ($r_2 = 2r_1$). An extended circle is denoted by $C_e(V)$, where V is the center of the extended circle. The nodes in an extended circle but not in a preferred circle are the second choice to be relay nodes. As shown in Fig. 4, a sensor node k in the extended circle V_3 is denoted by $k \in C_e(V_3)$.

Neighbor preferred circle: For the nodes in preferred circles, such as the node i in Fig. 4, its neighbor preferred circles are the circles centering around the charging points whose distances to the charging point V_1 are not larger than $\sqrt{2}d$. That is, neighbor preferred circles are the circles whose corresponding centers can constitute a square with V_1. As we can see in Fig. 4, the neighbor preferred circles of the node i are $C_p(V_2) \sim C_p(V_9)$. For the nodes not in preferred circles, such as nodes j and k, the neighbor preferred circles are the corresponding preferred circles on the vertices of the charging grid which the nodes j and k belong to. Therefore, the neighbor preferred circles of the nodes j and k are $C_p(V_1) \sim C_p(V_4)$.

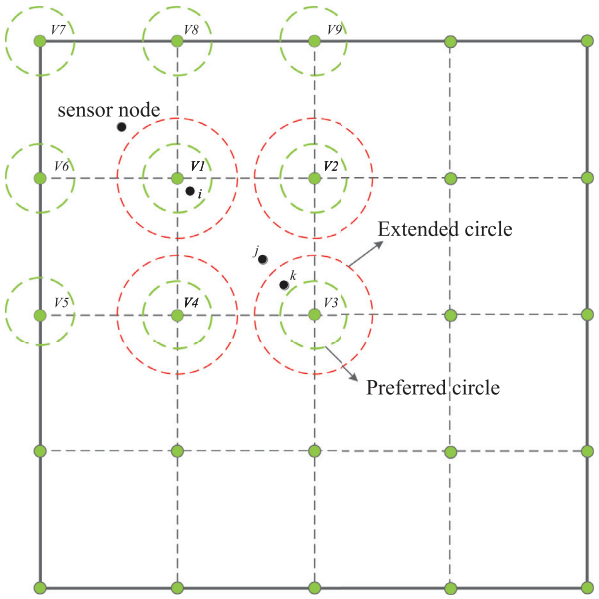

Fig. 4. Preferred circle and extended circle.

Neighbor extended circle: Similarly to neighbor preferred circles, for the nodes in a preferred circle, such as the node i in Fig. 4, its neighbor extended circles are the circles centering around the charging points whose distances to the charging point V_1 are not larger than $\sqrt{2}d$. For the nodes not in preferred circles, their neighbor extended circles are the corresponding extended circles on the vertices of the charging grid which they belong to. In other words, neighbor extended circles share the same centers with neighbor preferred circles. The difference is that the radius of a neighbor preferred circle is r_1, and the radius of a neighbor extended circle is $2r_1$.

Balance Factor: $BF_{ij} = \frac{d_{ij}}{p_{r_j}}$. Here, d_{ij} is the distance between the node i and its neighbor node j. p_{r_j} is the expected power j receives. The less the value of BF_{ij}, the more probable that the node j is selected as the next hop of i. It is reasonable, because for any neighbor node, if its distance to the node i is small, and its received power is large, it is more suitable to be the next-hop node. Selecting a node which has small balance factor is beneficial to balance energy consumption. That is why we call BF_{ij} the Balance Factor.

After deployment, each node in the network, for instance, the node i, broadcasts routing request packets to establish the routing path. The packets contain the node ID, location of the node i, and information about its neighbor preferred circles. Its neighbor nodes, for example the node j, which receive the packet, judge whether they themselves belong to the i's neighbor preferred circle. If yes, then j sends a packet to i, containing its ID, location,

and expected power P_{r_j} it can receive. Otherwise, j does not reply. After this process, i arranges the packets it receives, and selects the nodes which are closer to the Base Station. Then i calculates BF_{ij} for each of these nodes, and chooses the node which has the smallest value of BF_{ij} as its next hop node. Thus, if there exist neighbor nodes in the i's neighbor preferred circles, and they are closer to the Base Station than i, it can determine the next hop node.

If i fails to find its next hop during the process described above, it broadcasts packets to establish the routing path for the second time, containing its ID, location and information about its neighbor extended circles. Its neighbor nodes, such as node j, receive the packet, and check whether they belong to the i's neighbor extended circles. If yes, j sends a packet to i, containing its ID, location, and P_{r_j}. Otherwise, j does not reply. After this process, i arranges the packets it receives, and selects the nodes which are closer to the Base Station. Then i calculates BF_{ij} for each of these nodes, and chooses the one which has the smallest BF_{ij} as its next hop. After that, i sends a message to inform the node of being the next hop node.

If node i still cannot determine its next hop after the above two steps, it broadcasts packets to establish the routing path for the third time. Every its neighbor node replies with its ID and location. Then i chooses the node which is closer to the sink, and has the smallest distance to it, as its next hop node.

After the three steps described above, all the nodes in the network can determine their next hop nodes, and routing paths from them to the Base Station can be established. In the first and second steps, we choose the next hop nodes based on two factors: distances among nodes and received power. In the last step, we only consider distances among nodes. This is because the nodes in the preferred and extended circles can be replenished with more energy. For the other nodes that have lower energy, choosing the nearest node as the next hop helps reducing communication cost as much as possible. In other words, the main purpose of the routing protocol is to make the nodes closer to charging points take more responsibility to forward data packets. Hence, energy consumption in the charging grid area can be balanced to some degree.

3.2. Charging algorithm

Theoretically, nodes around the Base Station tend to consume more energy than those located far away from it, because they have to undertake more data transmission tasks. After a period of time, such nodes run out of energy first, which results in energy holes. Therefore, we propose a charging algorithm to solve the problem of energy unbalance caused by the routing protocol. A new traveling path is designed for a mobile charger, so that it can traverse all of the charging points, as seen in Fig. 5. When the mobile charger gets ready to replenish energy, it starts from the Base Station, moves along a predefined traveling trajectory, sojourns at charging points, and charges sensor nodes. As can be seen in Fig. 5, the traveling trajectory contains $\frac{L}{2\times d}$ square rings. For example, the charging points ① ~ ⑨ constitute the first square ring, and the charging points ⑩ ~ ㉕ constitute the second square ring. The

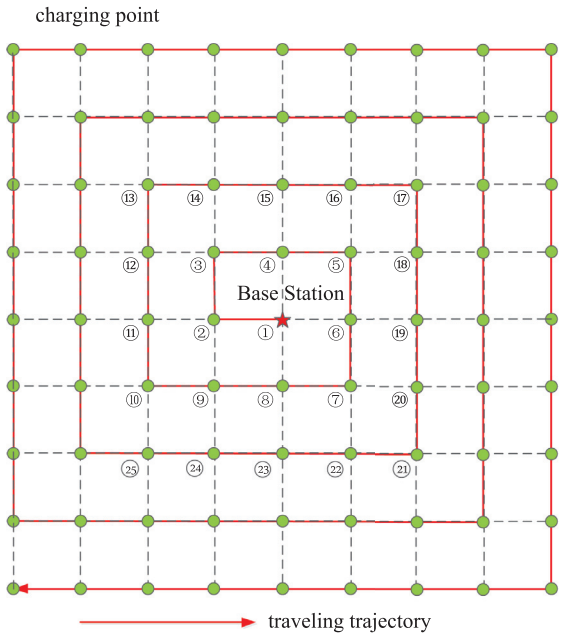

Fig. 5. Traveling trajectory of the mobile charger.

mobile charger moves from the innermost layer to the outermost layer gradually. The superiority of adopting this traveling path is that we can allocate different times to different square rings to control energy provisioned in different square rings in an easy way. A simple principle to allocate charging time is to make it proportional to energy consumption of the nodes around this square ring. This charging algorithm is designed to provide more energy to nodes which undertake more communication tasks, and have larger consumption rates.

Specifically, after a period of operating, the charger communicates with the Base Station to obtain the energy consumption rates of all sensor nodes, and enters the network at t_{en}. Further, the average energy consumption rate of every square ring $aveE_k$ can be acquired ($k \in [1, \frac{L}{2\times d}]$). Here, we set the threshold energy E_{th} for the nodes in the outermost square ring. Thus, we can calculate the total available time t_{total} that the mobile charger spends in the former $\frac{L}{2\times d} - 1$ square rings. Besides, the time that the mobile charger moves between charging points can be calculated as t_{travel}, so $t_{avai} = t_{total} - t_{travel}$ is the time that the charger can spend on replenishing energy. According to the analysis above, we can obtain:

$$\begin{cases} N_1 t_1 + N_2 t_2 + \cdots + N_{\frac{L}{2\times d}} t_{\frac{L}{2\times d}} = t_{avai} \\ \dfrac{t_1}{aveE_1} = \dfrac{t_2}{aveE_2} = \cdots = \dfrac{t_{\frac{L}{2\times d}}}{aveE_{\frac{L}{2\times d}}} \end{cases} \tag{4}$$

N_k represents the number of charging points in the square ring k. Based on this equation, the time t_k that should be spent on a certain square ring k can be calculated. For the outermost square ring, we can calculate the time allocated to it based on the former square rings as follows:

$$t_{\frac{L}{2\times d}} = \frac{t_1}{aveE_1} \times aveE_{\frac{L}{2\times d}} \tag{5}$$

Table 1
Parameter Configuration.

Parameters	Symbol	Value
Side Length of Area	L	$120m$
Side Length of Charging Grid	d	2, 3, 4, 5, 6(m)
Number of Nodes	N	300, 350, 400, 450, 500, 550
Communication Range	R_{co}	$15m$
Moving Speed	v_m	0.2, 0.6, 1, 1.4, 1.8(m/s)
Charging Range	R	$5m$
Initial Energy	E_0	$2J$
Radius of Preferred Circle	r_1	0.3, 0.4, 0.5, 0.6, 0.7, 0.8, 0.9, 1(m)
Transmitting Interval	T	$20s$
Entering Time	t_{en}	$60s$
Energy Threshold	E_{th}	1.4, 1.5, 1.6, 1.7, 1.8, 1.9(J)
Resolution	D	$6m$
Data Packet Size	n_1	$100bit$
Broadcast Packet Size	n_2	$25bit$

Having this, we have determined the charging time allocated to each charging point.

4. Simulation and evaluation

In this paper, we use MATLAB to simulate performance of the charging algorithm. In Table 1, we list specific parameters and their values. First, we conduct three groups of experiments to see how the values of d, E_{th}/E_0 and the radius of preferred circles r_1 affect charging performance of our proposed charging algorithm. Then, we compare in detail our proposed algorithm with the algorithm proposed in [14], the S-CURVES(ad), which also adopts a static traveling path, and was proved to be more superior than other charging algorithms via simulations. However, in [14], the authors just assume that the energy consumption rates of all nodes are equal. To compare the two algorithms in a fair way, we use one of the most widely used routing method, the greedy routing as its routing protocol. Specifically, every node chooses the node which is closer to the Base Station and has the smallest distance to it as its next hop node. 50 simulation runs are taken on average to reduce accidental errors.

In this paper, we choose three evaluation parameters: the average residual energy E_{ave}, standard deviation of energy E_{SD}, and survival rate η. They can be calculated according to Equations (6), (7) and (8).

$$E_{ave} = \frac{\sum_{i=1}^{N} E_{res_i}}{N} \tag{6}$$

$$E_{SD} = \sqrt{\frac{1}{N}\sum_{i=1}^{N}(E_{res_i} - E_{ave})^2} \tag{7}$$

$$\eta = N_{survive}/N \tag{8}$$

N is the total number of nodes, E_{res_i} represents the current energy of the node i, and $N_{survive}$ is the number of nodes which survive after the charger traverses the network once. As we can see from the formulations, the standard deviation of energy is to evaluate charging performance in energy balancing. The less E_{SD}, the better charging performance the charging algorithm can achieve.

4.1. Our proposed algorithm

In this part, the number of nodes is set to be 300, the moving speed of the mobile charger is $1m/s$. The values of d, E_{th}/E_0 and r_1 are changed to see how the proposed charging algorithm performs.

1) The effect of d: Apparently, as can be seen in Fig. 6(a), as d increases, the total length of the traveling path decreases, because it brings a smaller number of charging points. In Fig. 6(b), the average residual energy

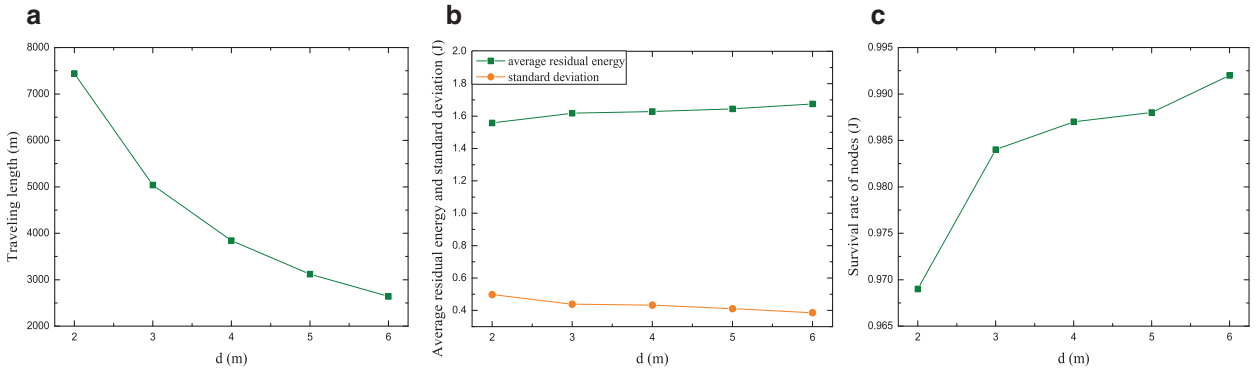

Fig. 6. (a) Traveling length VS d; (b) Average residual energy and standard deviation VS d; (c) Survival rate of nodes VS d.

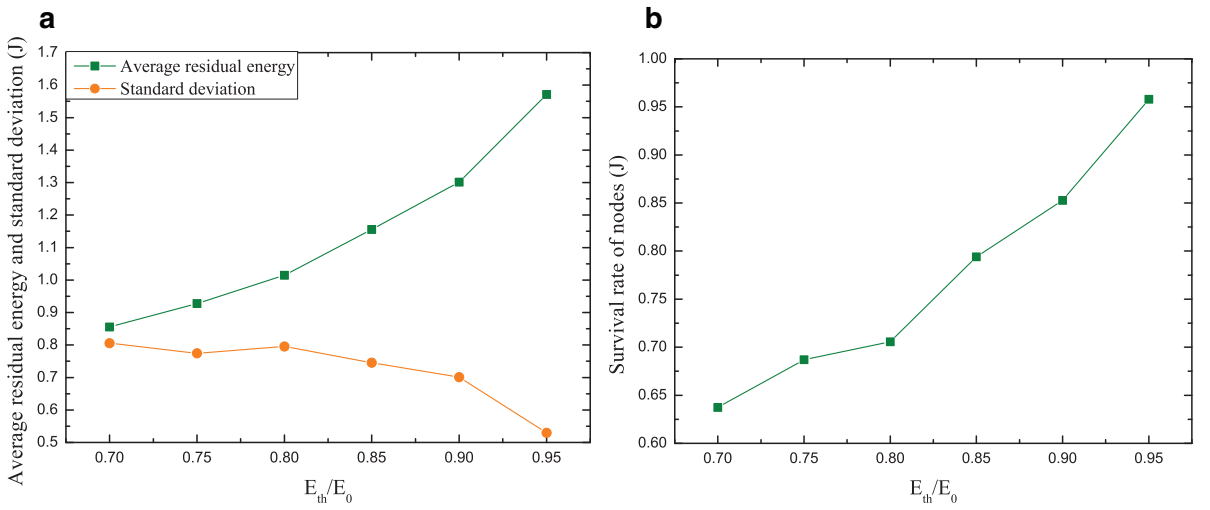

Fig. 7. (a) Average residual energy and standard deviation VS E_{th}/E_0 ; (b) Survival rate of nodes VS E_{th}/E_0.

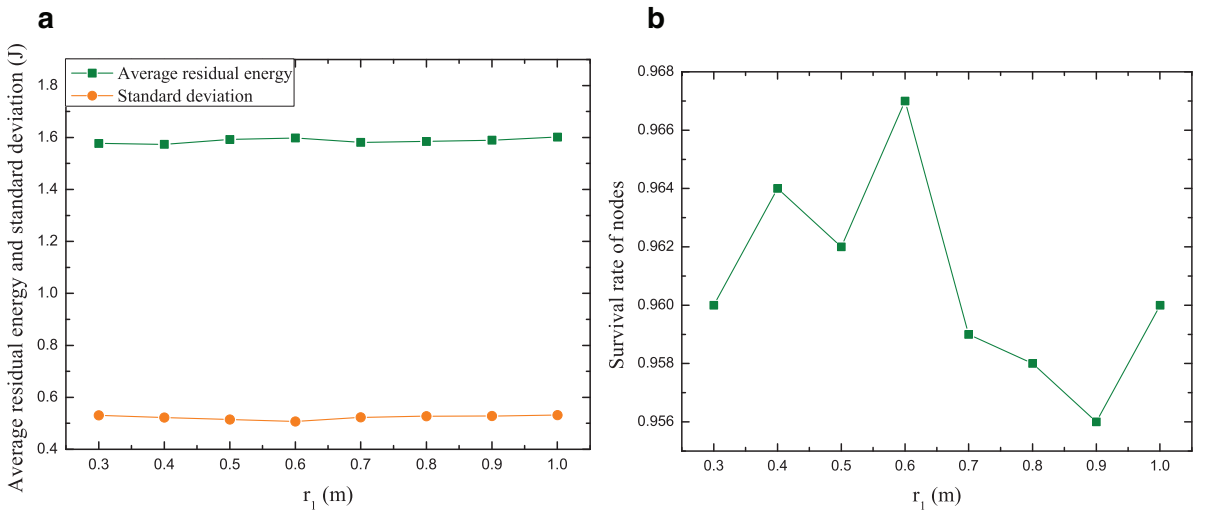

Fig. 8. (a) Average residual energy and standard deviation VS r_1 ; (b) Survival rate of nodes VS r_1.

becomes higher as d increases. This is reasonable, because as was analyzed before, the mobile charger wastes less time on traveling, and spends more time on charging. In addition, we note that the standard deviation of the average residual energy decreases as d increases. As mentioned before, a larger d means less square rings, and the charger spends more time on each square ring and each charging point, which is beneficial to the nodes close to charging points. These nodes take more responsibility to transmit data packets, therefore, they need to be replenished more energy. Hence, a more balanced energy distribution can be achieved when d increases. Therefore, in the following simulation parts, we set $d = 6m$.

2) The effect of E_{th}/E_0: In Fig. 7, we show how E_{th}/E_0 affects E_{ave}, E_{SD} and η. Combined with Fig. 7(a) and Fig. 7(b), we can observe that to some extent, the larger the energy threshold E_{th}, the better charging performance our proposed algorithm can achieve. As E_{th}/E_0 increases, the average residual energy increases, the standard deviation of the residual energy decreases, and the survival rate of nodes increases. This implies that a larger value of E_{th}/E_0 leads to a more balanced energy distribution and higher survival rates of nodes. It is reasonable, because when E_{th}/E_0 becomes larger, the charger has to spend less time on traversing the network and replenishing energy for nodes, to meet the energy demand of the nodes in the last square ring. That is, less energy is consumed during the procedure. Thus, more residual energy of nodes can be obtained. However, it should be noted that if the value E_{th}/E_0 is set too large, the time spent on energy provisioning will certainly be very limited, causing great waste of energy. Therefore, in the next simulation parts, we set E_{th}/E_0 to be 0.95.

3) The effect of r_1: In this experiment, we change the radius of the preferred circle r_1 from $0.3m$ to $1m$, with a step of $0.1m$. As shown in Fig. 8(a), as r_1 increases, the average residual energy and standard deviation change very little, and they achieve the highest value when r_1 is $0.6m$. In

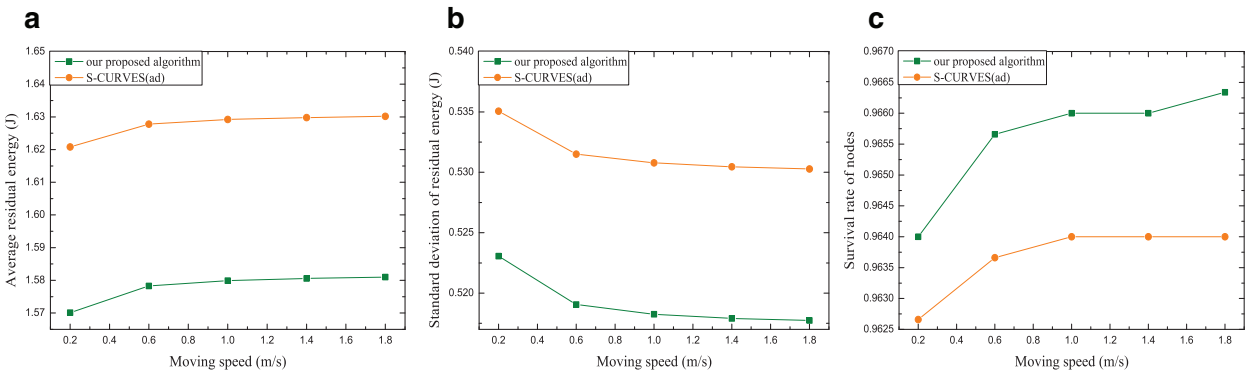

Fig. 9. (a) Average residual energy VS moving speed; (b) Standard deviation of residual energy VS moving speed; (c) Survival rate of nodes VS moving speed.

Fig. 8(b), we can see that, as r_1 changes, the survival rate of nodes changes within a limited range of $0.956 \sim 0.967$. As simulated in Fig. 3, provisioning energy drops rapidly when distances between nodes and charging points increase. In general, when the distance is larger than $1m$, energy that nodes can obtain is very small. Therefore, the radii of the preferred and extended circles cannot be very large. Otherwise, the routing protocol loses its meaning. Besides, the preferred and extended circles are relatively small, so increasing the radius has a small effect on charging performance.

4.2. Charging performance comparisons

In this subsection, we compare our proposed algorithm with the S-CURVES(ad). In both experiments, we set r_1 as $0.6m$, E_{th}/E_0 as 0.95, d as $6m$. In the first experiment, the moving speed of the mobile charger is changed from $0.2m$ to $1.8m$ with step $0.4m$. In the second one, we alter the number of nodes from 300 to 550 with step 50.

1) Charging performance comparison with varying v: Overall, increasing the moving speed of the mobile charger has a positive effect on charging performance. This is quite clear, as we can see in Fig. 9, the average residual energy and survival rate of nodes increase, and the standard deviation of the residual energy decreases for both algorithms. A faster moving speed implies that the charger wastes less time on traversing the network, and spares more time on provisioning energy, which is beneficial for prolonging the lifetime of nodes. In Fig. 9(a), we can see that the S-CURVES(ad) performs better than our algorithm in terms of average residual energy as the moving speed increases. This is due to the following reasons. On the one hand, the traveling length of the S-CURVES(ad) is shorter compared to the proposed algorithm. Hence, it wastes less time on traveling among charging points, and spares more time on replenishing energy. On the other hand, we can see that the average residual energy is lower than the initial energy, which means the energy consumption rate is larger than the energy provisioning rate. In our algorithm, the charger takes more time to replenish energy for nodes which undertake more communication tasks. And, at the same time, they usually consume more energy than what they get. Therefore, their residual energy is small. While in the S-CURVES(ad), the charger delivers equal energy to every charging point in the network. The nodes far away from the sink, they consume much less energy than the nodes near the Base Station, but they get equal energy. Thus, nodes in the S-CURVES(ad) can reserve more energy in general. In Fig. 9(b), we can see that our proposed algorithm outperforms the S-CURVES(ad) in balancing energy of nodes. This result is expected, because in our proposed algorithm, the charging time at each charging point is directly proportional to energy consumption rates of nodes around it. It verifies that our proposed algorithm works well in balancing energy. The survival rate of nodes is shown in Fig. 9(c). The survival rate of nodes in our proposed algorithm is higher than that of the S-CURVES(ad). As is analyzed above, although the S-CURVES(ad) performs well in terms of the average residual energy, it fails to achieve energy balance over the whole network. The nodes close to the Base Station or with low energy, while being chosen to take more communication tasks, are more likely to run out of energy and die early. Compared to the S-CURVES(ad), our proposed grid-based joint routing and charging algorithm overcomes the drawback in a better way.

2) Charging performance comparison with varying N: Fig. 10(a) shows how the average residual energy changes when the number of nodes increases. It can be observed from this picture that for both algorithms, the average residual energy is progressively increased as the number of nodes augments, and the magnitude of increase is very small. As the network becomes denser, the number of nodes which get more energy becomes larger under the same energy provisioning conditions. Fig. 10(b) verifies superiority of our proposed algorithm in terms of energy balance. The standard deviation of the residual energy in our proposed algorithm is clearly smaller than that of the S-CURVES(ad). In Fig. 10(c), we note that, as the number of nodes increases, more nodes use up energy due to the fact that the energy consumption rate of nodes is larger than the energy provisioning rate. Therefore, the survival rate of nodes decreases. The two algorithms have almost the same performance in the survival rate of nodes when the number of nodes is from 300 or 350. However,

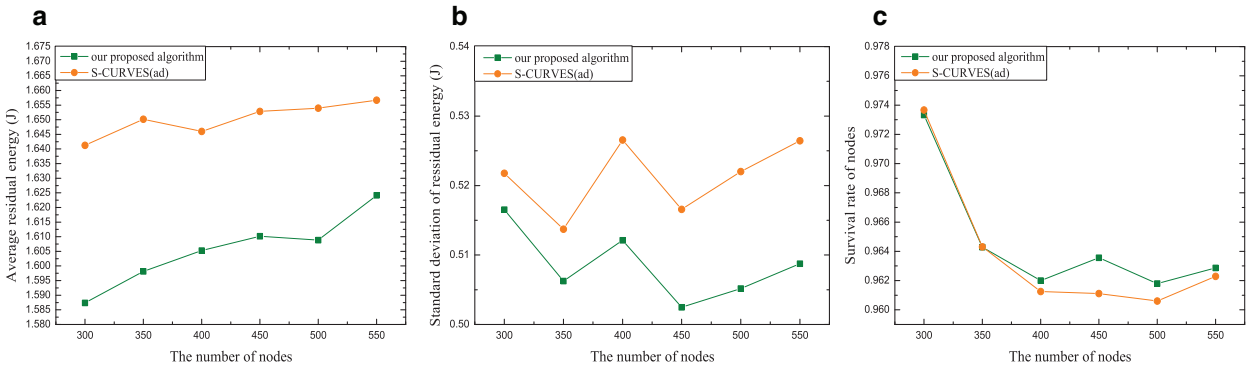

Fig. 10. (a) Average residual energy VS the number of nodes; (b) Standard deviation of residual energy Vs the number of nodes; (c) Survival rate of nodes VS the number of nodes.

when the number of nodes increases, the survival rate of nodes in our algorithm becomes higher than that of the S-CURVES(ad). This can be explained as follows. When the network becomes denser, there are more nodes in preferred and extended circles, and more nodes are likely to choose these nodes as next-hop nodes. And this is beneficial to achieve energy balance. Accordingly, the survival rate of our proposed algorithm becomes higher than that of the S-CURVES(ad) as N increases.

5. Conclusion

In this paper, we propose a grid-based joint routing and charging algorithm for IWRSNs. Simulation results show its superiority in achieving energy balance and improving survival rates of nodes in the network by comparing to the S-CURVES(ad) algorithm. It benefits from the following two aspects. 1) The routing protocol is designed based on the charging characteristics within charging grids, which brings energy balance in the local grid area. 2) The charging time at different charging points is decided by energy consumption rates of nodes around them, which leads to energy balance in the global network. On this premise, energy balance in the network and longer lifetimes of nodes can be achieved.

In the future, a more efficient traveling path can be designed, achieving larger survival rates of nodes. Further, an uneven distribution of nodes and barriers in the network should be taken into consideration.

Acknowledgements

The work is supported by “Qing Lan Project” and “the National Natural Science Foundation of China”, Grant 61572172, and “Natural Science Foundation of Jiangsu Province of China”, No.BK20140248.

References

[1] P.T.A. Quang, D.-S. Kim, Enhancing real-time delivery of gradient routing for industrial wireless sensor networks[J], Industrial Informatics, IEEE Transactions on 8 (5) (2012) 61–68.
[2] V.C. Gungor, G.P. Hancke, Industrial wireless sensor networks: Challenges, design principles, and technical approaches, IEEE TRANSACTIONS ON INDUSTRIAL ELECTRONICS 56 (10) (2009) 4258–4265.
[3] K. Mikhaylov, J. Tervonen, J. Heikkilä, J. Känsäkoski, Wireless sensor networks in industrial environment: Real-life evaluation results[C], Future Internet Communications (BCFIC) (2012) 1–7.
[4] M. Chen, J. Wan, González, X. Liao, V.C.M. Leung, A survey of recent developments in home M2M networks, IEEE Communications Surveys and Tutorials 16 (1) (2014) 98–114.
[5] J. Wan, C. Zou, S. Ullah, C.-F. Lai, M. Zhou, X. Wang, Cloud-enabled wireless body area networks for pervasive healthcare, IEEE Network 27 (5) (2013) 56–61.
[6] G. Han, Y. Dong, H. Guo, L. Shu, D. Wu, Cross-layer optimized routing in wireless sensor networks with duty-cycle and energy harvesting, Wireless Communications and Mobile Computing (2015), doi:10.1002/wcm.2468.
[7] G. Han, H. Guo, C. Zhang, L. Shu, Parameter optimisation in duty-cycled wireless sensor networks under expected network lifetime., International Journal of Ad Hoc and Ubiquitous Computing 15 (1-3) (2014a) 57–67.
[8] G. Han, X. Jiang, A. Qian, J.J.P.C. Rodrigues, L. Cheng, A comparative study of routing protocols in heterogeneous wireless sensor networks, The Scientific World Journal 2014 (2014b). Article ID 455415
[9] K. Li, H. Luan, C.-C. Shen, Qi-ferry: Energy-constrained wireless charging in wireless sensor networks[C], IEEE Wireless Communications and Networking Conference: Mobile and Wireless Networks (2012) 2515–2520.
[10] L. He, Z. Yang, J. Pan, L. Cai, J. Xu, Evaluating service disciplines for mobile elements in wireless ad hoc sensor networks, In INFOCOM, 2012 Proceedings IEEE (2012) 576–584.
[11] F. Jiang, S. He, P. Cheng, J. Chen, On optimal scheduling in wireless rechargeable sensor networks for stochastic event capture, IEEE 8th International Conference on MASS (2011) 69–74.
[12] L. Xie, Y. Shi, Y.T. Hou, S. Member, H.D. Sherali, Making sensor networks immortal: An energy-renewal approach with wireless power transfer, IEEE/ACM TRANSACTIONS ON NETWORKING 20 (6) (2012) 1748–1761.
[13] M. Zhao, J. Li, Y. Yang, Joint mobile energy replenishment and data gathering in wireless rechargeable sensor networks, Proceedings of the 23rd International Teletraffic Congress (2011) 238–245.
[14] G. Han, A. Qian, L. Liu, J. Jiang, C. Zhu, Impacts of traveling paths on energy provisioning for industrial wireless rechargeable sensor networks, Microprocessors and Microsystems (2015), doi:10.1016/j.micpro.2015.07.002.
[15] S. He, J. Chen, F. Jiang, D.K.Y. Yau, G. Xing, Y. Sun, Energy provisioning in wireless rechargeable sensor networks, Mobile Computing, IEEE Transactions on 12 (2013) 1931–1942.
[16] J.-H. Liao, C.-M. Hong, J.-R. Jiang, An adaptive algorithm for charger deployment optimization in wireless rechargeable sensor networks, ICS (2014).
[17] R. Beigel, J. Wu, H. Zheng, On optimal scheduling of multiple mobile chargers in wireless sensor networks, Proceedings of the first international workshop on Mobile sensing, computing and communication (2014) 1–6.
[18] C.M.A. c, S. Nikoletseas, T.P. Raptis, Wireless energy transfer in sensor networks with adaptive, limited knowledge protocols, Computer Networks (2014) 113–141.
[19] Z. Li, Y. Peng, W. Zhang, D. Qiao, Study of joint routing and wireless charging strategies in sensor networks, Wireless Algorithms, Systems, and Application 6221 (2010) 125–135.

[20] L. Fu, P. Cheng, Y. Gu, J. Chen, T. He, Minimizing charging delay in wireless rechargeable sensor networks, INFOCOM, 2013 Proceedings IEEE (2013) 2922–2930.
[21] P. Cheng, S. He, F. Jiang, Y. Gu, J. Chen, Optimal scheduling for quality of monitoring in wireless rechargeable sensor networks[J], Wireless Communications, IEEE Transactions on 12 (6) (2013) 3072–3084.
[22] G. Han, J. Chao, C. Zhang, L. Shu, Q. Li, The impacts of mobility models on DV-hop based localization in mobile wireless sensor networks, Journal of Network and Computer Applications 42 (6) (2014a) 70–79.
[23] G. Han, C. Zhang, L. Shu, J.J.P.C. Rodrigues, J. Lloret, A mobile anchor assisted localization algorithm based on regular hexagon in wireless sensor networks, The Scientific World Journal 2014 (2014b). Article ID 219371
[24] G. Han, H. Xu, J. Jiang, L. Shu, N. Chilamkurti, The insights of localization through mobile anchor nodes in wireless sensor networks with irregular radio, KSII Transactions on Internet and Information Systems (TIIS) 6 (11) (2012) 2992–3007.
[25] O. Younis, S. Fahmy, HEED: a hybrid, energy-efficient, distributed clustering approach for ad hoc sensor networks[J], Mobile Computing, IEEE Transactions on 3 (4) (2004) 366–379.

Guangjie Han is currently a Professor with the Department of Information and Communication System, Hohai University, Changzhou, China. He received the Ph.D. degree from Northeastern University, Shenyang, China, in 2004. From 2004 to 2006, he was a Product Manager for the ZTE Company. In February 2008, he finished his work as a Postdoctoral Researcher with the Department of Computer Science, Chonnam National University, Gwangju, Korea. From October 2010 to 2011, he was a Visiting Research Scholar with Osaka University, Suita, Japan. He is the author of over 180 papers published in related international conference proceedings and journals, and is the holder of 75 patents. His current research interests include sensor networks, computer communications, mobile cloud computing, and multimedia communication and security. Dr. Han has served as a Cochair for more than 30 international conferences/workshops and as a Technical Program Committee member of more than 100 conferences. He has served on the Editorial Boards of up to 16 international journals, including the *International Journal of Ad Hoc and Ubiquitous Computing, Journal of Internet Technology*and *KSII Transactions on Internet and Information Systems.*He has served as a Reviewer of more than 50 journals. He had been awarded the ComManTel 2014, ComComAP 2014 and Chinacom 2014 Best Paper Awards. He is a member of IEEE and ACM.

Aihua Qian is currently persuing her Master degree from Department of Information & Communication Engineering at the Hohai University, China. She received her B.S. degree in Information & Communication Engineering from Hohai University, China, in 2013. Her current research interests are wireless charging for Wireless Sensor Networks.

Jinfang Jiang received the BS degree in information & communication engineering from Hohai University, China, in 2009. She is currently working toward the PhD degree from the Department of Information & Communication System at Hohai University, China. Her current research interests are security and localization for sensor networks.

Ning Sun received the PhD degree for Computer Science from The Chungbuk National University, Korea, in February 2013. Since then, she has been a lecturer in the Department of IOT Engineering at Hohai University, China. Her research interests are in the design and evaluation of network architectures and protocols. She is currently investigating wireless sensor networks, Internet of Things and network security.

Li Liu is currently persuing his Master degree from Department of Information & Communication Engineering at the Hohai University, China. He received his B.S. degree in Information & Communication Engineering from Hohai University, China, in 2014. His current research interests are coverage and connectivity for Wireless Sensor Networks.